

NONLINEAR DEFORMATION AND STABILITY OF OVAL CYLINDRICAL SHELLS UNDER COMBINED LOADING

L. P. Zheleznov, V. V. Kabanov,
and D. V. Boiko

UDC 539.3:534.1

A study is made of the stability of cylindrical shells of oval cross section loaded by a shear force combined with torsional and bending moments. The variational method of finite elements in displacements is used. The subcritical stress–strain state of the shells is considered momental and nonlinear. The effects of the nonlinearity of shell deformation and shell ovalization on the critical load and buckling mode are determined.

Key words: *oval cylindrical shells, bending by a shear force with a torsional or bending moment, nonlinear deformation, stability, finite element method.*

Introduction. The stability of noncircular shells has been studied insufficiently compared to circular shells. Most of the studies of this issue have been performed in a first approximation using the classical linear theory of shells and some assumptions: momentless subcritical stress state, deformation simplifications, etc. The error of the linear theory, as a rule, has not been estimated; this theory proves insufficiently reliable in some cases because shells, for example, aircraft fuselages are thin-shell structures and are deformed mainly nonlinearly under large displacements. At present, pressurized fuselage structures with oval and elliptic cross sections have been developed. Such pressurized fuselage cabins provide a more effective use of the fuselage interior for passenger accommodation. Buckling of the pressurized fuselage skin is inadmissible since it reduces the fuselage stiffness and strength, and repeated instability can lead to crack formation and depressurization of the fuselage cabin. The case of loading of oval cylindrical shells considered here has not been studied even in the classical formulation.

Investigation of Nonlinear Deformation and Stability of a Shell. We study the problem of nonlinear deformation and stability of a cantilever fitted ($u = v = w = w_x = 0$; u , v , and w are the shear displacements and deflection of the shell; the subscript x denotes differentiation over the coordinate x) cylindrical shell of oval cross section acted upon by a shear force Q , a torsional moment M_t , and a bending moment M (Fig. 1). The loaded edge of the shell was stiffened by a rib which is rigid in its plane. We replace the action of the torsional moment by the action of linear boundary shear forces $T = M_t/(2\omega)$ (ω is the area bounded by the cross-sectional contour of the shell), the action of the shear force by statically equivalent shear forces $T = QS/J$ (S is the static moment of the sheared part of the cross section and J is the moment of inertia of the shell cross section with respect to the axis AA), and the action of the bending moment by the action of linear axial forces $T = Mz_1/J$, which are nonuniform along the shell direction (z_1 is the distance from the points of the shell contour to the horizontal axis AA). The shell has length $L = 1100$ mm, thickness $h = 5$ mm, elastic modulus $E = 7 \cdot 10^4$ MPa, Poisson ratio $\nu = 0.3$, equiperimetric radius (the radius of a circular shell with perimeter equal to the perimeter of the oval shell) $R_0 = 1000$ mm.

Let us consider an oval with half-axes a and b (see Fig. 1) which is constructed of two pairs of circles as follows. We draw a circle of radius a with center O until the intersection with the half-axis b . Then, we draw a circle of radius $a - b$ until the intersection with the straight line AB. We bisect the segment AC and draw a perpendicular

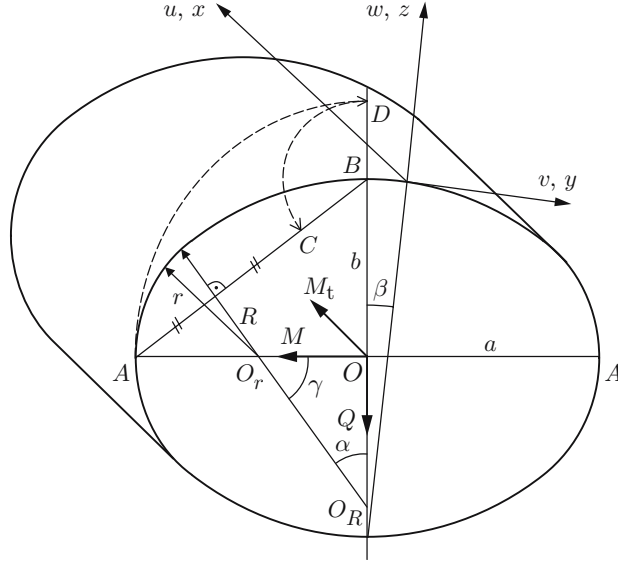


Fig. 1. Diagram of construction of an oval.

TABLE 1

\bar{a}	a	R	r	α , deg
1.00	1000.00	1000.00	1000.000	45.00
1.25	1106.48	1311.20	765.061	38.66
1.67	1224.42	1863.63	547.033	30.96
2.50	1348.47	3044.53	346.410	21.80

to it. We draw arcs of circles of small r and large R radii from the centers O_r and O_R , respectively. The point of conjugation of the arcs of the circles is determined by the angle α . From the conditions of construction of the oval, we have its geometrical characteristics

$$r = a \frac{1 + k^2 - \sqrt{1 + k^2}}{1 + k - \sqrt{1 + k^2}}, \quad R = a \frac{1 - k(\sqrt{1 + k^2} - k)}{1 + k - \sqrt{1 + k^2}}, \quad k = \tan \alpha = \frac{b}{a}, \quad \bar{a} = \frac{1}{k}.$$

The perimeter of the oval is $P = 4(R\alpha + r\gamma)$, where $\gamma = \pi/2 - \alpha$. Table 1 give values of a , R , r , and α versus the shell ovalization parameter \bar{a} .

The problem was studied numerically using the variational displacement finite-element method developed in [1–3].

Because of the symmetry of the shell and load, the calculations were performed for half of the shell, which was partitioned by a finite-element grid $m \times n = 26 \times 77$.

For equiparametric oval shells in the case of separate action of the loads, Fig. 2 shows curves of the parameters $k_{m0} = M_0^*/M_0$, $k_{p0} = M_{t0}^*/M_{t0}$, $k_{r0} = Q_0^*/Q_0$ versus the parameter \bar{a} for the case of linear and nonlinear initial stress–strain states. Here Q_0^* , M_{t0}^* , and M_0^* are the critical values of the shear force and the torsional and bending moments; $Q_0 = \pi R_0 S_b$, $M_{t0} = 2\pi C R_0^2 S_b$, and $M_0 = \pi E R_0 h^2 / \sqrt{3(1 - \nu^2)}$ are the critical classical values of the shear force and the torsional and bending moments for a circular cylindrical shell of radius R_0 ; $S_b = 0.78 E h (h/R_0)^{5/4} (R_0/L)^{1/2}$; $C = 0.953$.

It is evident that, in most of the range of \bar{a} , the critical loads of the oval shells are smaller than the critical loads of equiparametric circular shells. In the case of transverse bending in the range of the ovalization parameter $1.0 < \bar{a} < 1.3$ and in the case of bending by the moment in the range $0.6 < \bar{a} < 1.0$, the critical loads of the oval shells are larger than the critical loads of the circular shells. In these cases, the mass of the oval shells are smaller than the mass of the circular equiparametric shells. The effect of the nonlinearity of the initial stress–strain state is insignificant (the difference between the strains and stresses is about 10%) and depends weakly on the parameter \bar{a} .

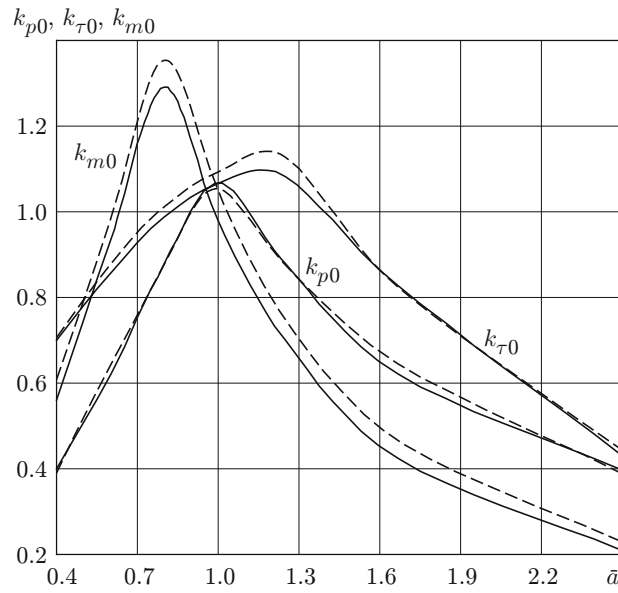


Fig. 2. Parameters k_{p0} , $k_{\tau0}$, and k_{m0} versus the parameter \bar{a} in the case of separate action of the loads: the dashed curves refer to the linear initial stress-strain state; the solid curves refer to the nonlinear initial stress-strain state.

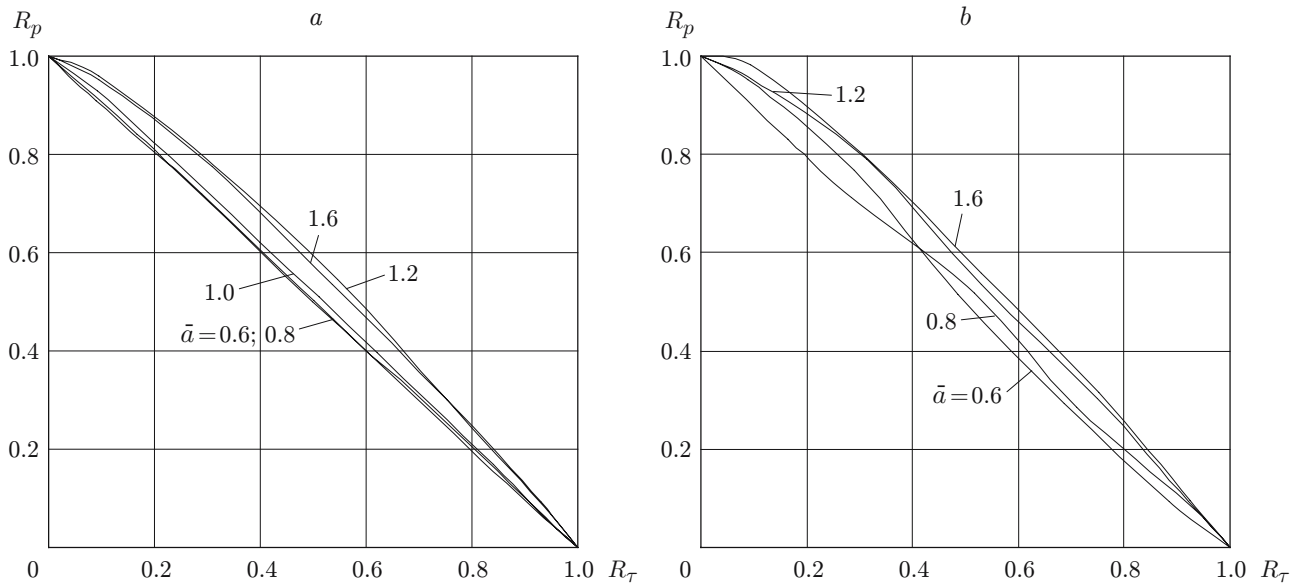


Fig. 3. Curve of $R_p(R_\tau)$: (a) linear initial stress-strain state; (b) nonlinear initial stress-strain state.

Figure 3 shows curves of $R_p(R_\tau)$ for the initial linear (Fig. 3a) and nonlinear (Fig. 3b) stress-strain states for various values of the parameter \bar{a} ($R_\tau = k_\tau/k_{\tau0} = Q^*/Q_0^*$; $R_p = k_p/k_{p0} = M_t^*/M_{k0}^*$; k_τ , k_p , Q^* , and M_t^* are the critical values of the parameters and loads for combined loading; $k_{\tau0}$, k_{p0} , Q_0^* , and M_{k0}^* are the critical values of the parameters and loads for separate loading). It is evident that the curves are convex, and their curvature changes weakly with a change of the parameter \bar{a} .

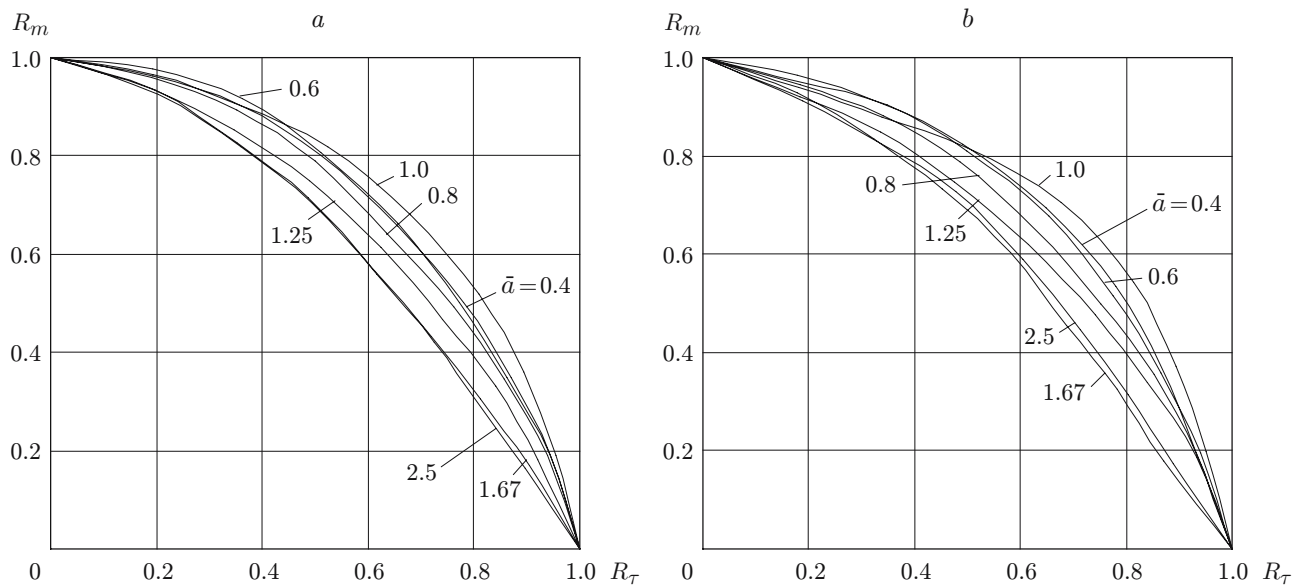


Fig. 4. Curve of $R_m(R_\tau)$: (a) linear initial stress–strain state; (b) nonlinear initial stress–strain state.

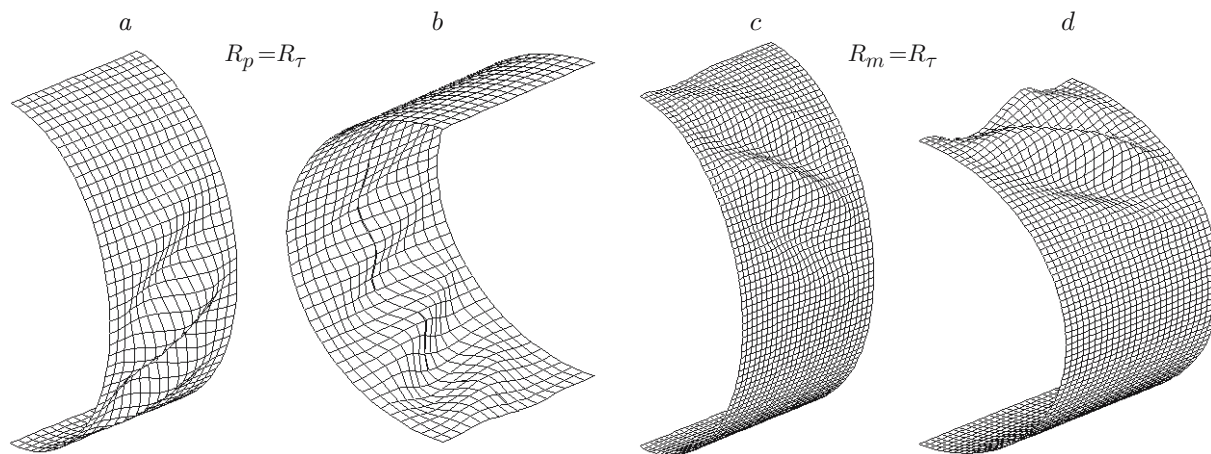


Fig. 5. Shell buckling modes for $\bar{a} = 0.8$ (a and c) and $\bar{a} = 1.25$ (b and d) for the cases of simultaneous action of the shear force and the torsional moment (a and b) and the shear force and the bending moment (c and d).

Figure 4 shows curves of $R_m(R_\tau)$ for the linear (Fig. 4a) and nonlinear (Fig. 4b) initial stress–strain states for various values of the parameter \bar{a} ($R_\tau = k_\tau/k_{\tau 0} = Q^*/Q_0^*$; $R_m = k_m/k_{m0} = M^*/M_0^*$; k_τ , k_m , Q^* , and M^* are the critical values of the parameters and loads for combined loading; $k_{\tau 0}$, k_{m0} , Q_0^* , and M_0^* are the critical values of the parameters and loads for separate loading). It is evident that the curves are convex and that their curvature decreases with increasing parameter \bar{a} .

Figure 5 shows some characteristic buckling modes of half of the shells for the values of the parameter $\bar{a} = 0.80$ and 1.25 . It is evident that the shell buckling mode depends greatly on the parameters \bar{a} , R_p , R_τ , and R_m . For $R_p = R_\tau$, the shells, as a rule, buckle in the region of the maximum shear forces with the formation of two inclined folds in the zone of small curvature of the shells. For $R_m = R_\tau$, the vertically elongated (high) shells ($\bar{a} = 0.8$) buckle in a shear mode, and horizontally elongated (low) shells ($\bar{a} = 1.25$) buckle in a mixed mode under the action of normal and shear forces.

REFERENCES

1. L. P. Zheleznov and V. V. Kabanov, "Finite element and algorithm for studying the nonlinear deformation and stability of noncircular cylindrical shells," in: *Applied Problems of the Mechanics of Thin-Shell Structures* [in Russian], Uzd. Mosk. Univ., Moscow (2000), pp. 120–127.
2. L. P. Zheleznov and V. V. Kabanov, "Nonlinear deformation and stability of noncircular cylindrical shells under internal pressure and axial compression," *J. Appl. Mech. Tech. Phys.*, **43**, No. 4, 617–621 (2002).
3. L. P. Zheleznov, V. V. Kabanov, and D. V. Boiko, "Nonlinear deformation and stability of oval cylindrical shells under pure bending and internal pressure," *J. Appl. Mech. Tech. Phys.*, **47**, No. 3, 406–411 (2006).